Journal of the Geological Society, London, Vol. **161**, 2004, pp. 67–79. Printed in Great Britain.

Microstructure and lattice preferred orientation of calcite mylonites at the base of the southern Urals accretionary prism

F. J. FERNÁNDEZ[1], D. BROWN[2], J. ÁLVAREZ-MARRÓN[2], D. J. PRIOR[3] & A. PÉREZ-ESTAÚN[2]

[1]*Departamento de Geología, Universidad de Oviedo, C/ Jesús Arias de Velasco, s/n 33005 Oviedo, Spain (e-mail: brojos@geol.uniovi.es)*

[2]*Instituto de Ciencias de la Tierra 'Jaume Almera' CSIC, Lluís Sollé i Sabarís, s/n 08028 Barcelona, Spain*

[3]*Department of Earth Sciences, Liverpool University, Liverpool L69 3GP UK*

Abstract: Emplacement of the southern Urals accretionary complex onto the East European Craton involved off-scraping of shallow marine limestones from the continental margin and their underplating to the base of the accretionary complex during the final stages of arc–continent collision. These limestones underwent localized ductile to semi-brittle deformation at upper-crustal levels, at temperatures close to 200 °C. Field observations, macroscopic fabric elements and crystallographic preferred orientations indicate a heterogeneous distribution of the deformation. Measurements from twinned calcite grains indicate that peak differential stress conditions during deformation attained *c*. 230 ± 40 MPa. These differential stress conditions are further supported by the small size of both recrystallized and twinned calcite grains. Twinning and intracrystalline slip were the major contributors to the bulk deformation and lattice preferred orientation (LPO) formation. LPO evolved with progressive strain, from an initial constrictional fabric that is consistent with the macroscopic mineral lineation as the dominant macroscopic fabric element to a *c*-axis maximum normal to foliation as the rock underwent dynamic recrystallization and grain refinement during progressive simple shear.

Keywords: Timirovo duplex, calcite, twinning, microstructure, stress.

Mylonitic limestones are particularly useful rocks for studying deformation mechanisms and fabrics in carbonate rocks. This is largely because calcite has crystallographic and optical characteristics that allow detailed analyses of textures, fabrics and fabric development. In addition, calcite fabrics have been extensively studied experimentally in a number of deformation regimes and over a wide range of temperature and pressure conditions (e.g. Turner *et al*. 1956; Wenk *et al*. 1973; Rutter 1974, 1995; Kern & Wenk 1983; Wagner *et al*. 1982; Schmid *et al*. 1987; Casey *et al*. 1998; Pieri *et al*. 2001). Natural examples of calc-mylonites have been described from several locations, and comparison of these with experimental data has provided important insights into the deformation processes that occur in a variety of tectonic settings (e.g. Schmid *et al*. 1981; Dietrich & Song 1984; De Bresser 1989; Ratschbacher *et al*. 1991; Erskine *et al*. 1993; Busch & van der Pluijm 1995). These studies show that crystallographic and grain shape fabric analyses can help determine the strain path of a shear zone, and provide information about the effects of mechanical reworking and overprinting of fabrics, as well as estimates of the environmental conditions during deformation.

The southern Urals of Russia are a superb example of an accretionary complex (Fig. 1), which was emplaced westward over the subducting continental crust of the East European Craton during accretion of the Magnitogorsk volcanic arc during the Mid- and Late Devonian (Brown *et al*. 1998; Brown & Spadea 1999; Álvarez-Marrón *et al*. 2000). Along much of its western margin, the base of the accretionary complex is composed of highly deformed Devonian limestones that were scraped off the subducting East European Craton (Brown *et al*. 1997, 1998; Álvarez-Marrón *et al*. 2000). Lattice preferred orientations (LPOs) and microstructural analyses of calcite from localized high-strain zones developed within the limestone allow constraints to be placed on the deformation mechanisms and pressure–temperature conditions during deformation.

Geological framework

Beginning in the Early Devonian, the tectonic setting in the southern Uralides was dominated by the development of the Magnitogorsk volcanic arc above an east-dipping (current co-ordinates) intra-oceanic subduction zone, while the easternmost East European Craton was evolving as a passive continental margin (e.g. Zonenshain *et al*. 1990; Puchkov 1997; Brown *et al*. 1998; Brown & Spadea 1999). With the entrance of the East European Craton continental crust into the subduction zone during the Mid-Devonian, volcanism in the Magnitogorsk arc shifted eastward and continued until the end of the Devonian–Early Carboniferous (Puchkov 1997). Continental slope and platform sediments were scraped off the subducting continental crust and together with arc-derived volcaniclastic sediments formed an accretionary complex (Brown *et al*. 1998; Brown & Spadea 1999).

The accretionary complex (Fig. 1) is composed of Silurian to Mid-Devonian continental slope and platform sedimentary rocks (Suvanyak Complex and Timirovo thrust system) that were detached from the East European Craton, and are overthrust by *c*. 5 km of late Frasnian and Famennian syncollisional volcaniclastic turbidites, sourced largely from the Magnitogorsk arc (Zilair Nappe) (e.g. Puchkov 1997; Brown *et al*. 1998). These units are flanked to the east by eclogite- and blueschist-bearing gneisses of the Maksutovo Complex that record a peak metamorphic age of *c*. 380–370 Ma (Matte *et al*. 1993; Beane & Connelly 2000; Glodny *et al*. 2002). The highest structural level in the accretionary wedge is the Kraka lherzolite massif

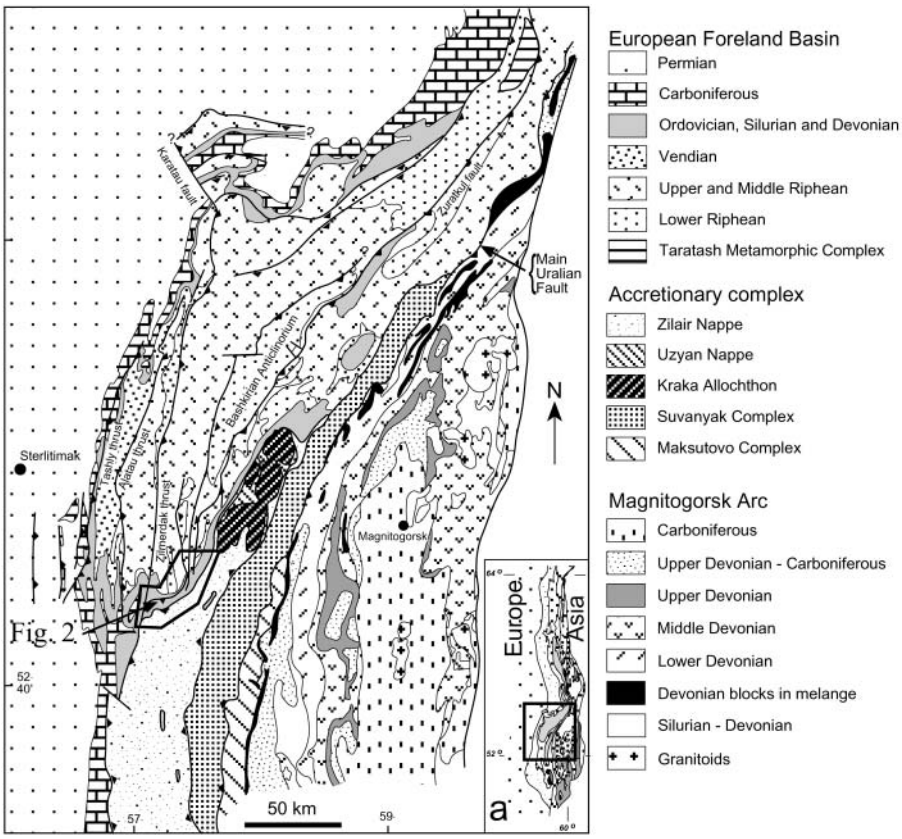

Fig. 1. Geological map of the southern Urals. The location is shown in the inset. The location of Figure 2 is also shown.

(Savalieva *et al*. 1997). The accretionary wedge is sutured to the Magnitogorsk arc along the east-dipping Main Uralian fault zone, a *c*. 10 km wide mélange that contains several ultramafic fragments.

The Timirovo thrust system

The Timirovo thrust system (Figs 1 and 2), which is the focus of this paper, crops out continuously along the Belaya River for nearly 100 km, from south of the village of Ctarosubkhangulovo to Beloresk in the north (Fig. 1). It developed during the final stages of emplacement of the accretionary complex, and forms a west-vergent thrust stack composed of highly deformed and sheared Devonian reef limestone structurally beneath the Zilair Nappe (Brown *et al*. 1997). Locally, near the village of Timirovo, the limestones are intercalated with arkosic sandstones. The roof thrust of the Timirovo thrust system is the Zilair Thrust, which consists of a 300–500 m thick calc-mylonite (Álvarez-Marrón *et al*. 2000). The rocks within the thrust sheets are imbricated along ductile shear zones that are 1 m to several tens of metres thick. It is difficult to follow the shear zones laterally away from river sections because of the thick forest cover in the area. Limestones within the calc-mylonite band show foliations with different degrees of development including zones of low deformation where the original bioclastic fabrics are preserved. Shear zones display a well-developed gently ESE-dipping foliation and an east-plunging lineation (Fig. 2) that, together with widespread kinematic indicators such as σ and δ clasts, indicate a top-to-the-WSW sense of movement (Fig. 3). The mesoscopic foliation in the rocks is defined by variations in grain size and, in some places, by phyllonitization and/or secondary dolomitization. The Timirovo thrust system is locally cut by a late, west-vergent brittle thrust related to the Permian formation of the foreland thrust and fold belt. These faults are not considered in analyses that follow.

The grade of metamorphism in the Timirovo thrust system has not been determined directly. The regional conodont colour alteration index is 4.5–5 (V. Barishev, pers. comm.), suggesting a temperature range of *c*. 250–300 °C. Illite crystallinity measurements carried out on samples in the overlying Zilair Nappe indicate that the metamorphic grade along the western margin of the nappe does not quite reach the chlorite zone (Bastida *et al*. 1997). During this study, however, chlorite associated with the final stages of deformation has been identified in the limestone and arkosic sandstone of the Timirovo thrust system.

Microstructures in the variably deformed limestones

The heterogeneous deformation of the limestones within the Timirovo thrust system is outlined in outcrop by highly deformed bands among less deformed bands. Optical analysis of thin sections reveals a large variety of microstructures covering the entire range of fault-related rocks from cataclasites to ultramylonites. We have selected three main types of microstructures showing increasing degrees of deformation that may serve as type lithologies for descriptive purposes. A large range of microstructures intermediate to these type members can be found. Unless otherwise stated, microstructures are described for sections cut normal to macroscopic foliation and parallel to lineation defined by individual grains or clusters of grains.

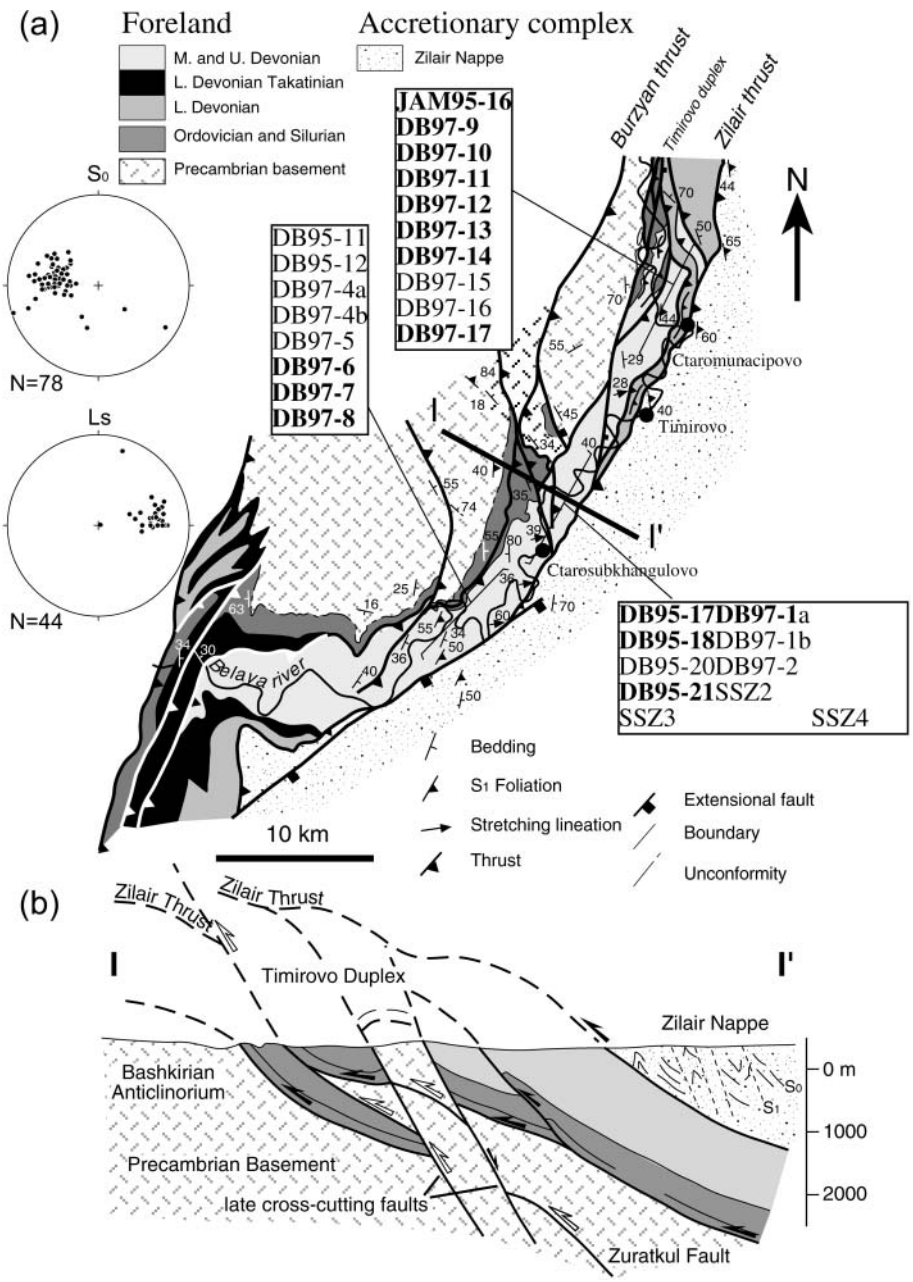

Fig. 2. (**a**) Geological map of the study area. The units of the foreland and the accretionary complex, and the sample locations, are indicated. Samples used for crystallographic fabrics are shown in bold type and those used for microstructural or palaeostress analyses in non-bold type. Bedding (S_0) and mylonitic foliation are parallel and Ls is the stretching lineation. (**b**) Cross-section I–I′ (location is given in (**a**)) shows the Zilair Thrust and its footwall.

Type I microstructures

Type I microstructures are widely distributed in outcrop, and are characterized by a weak fabric with heterogeneous grain size. Calcite veins and a weak grain shape fabric in the matrix are present. The micro-veins are filled by coarse-grained calcite or alternatively by cataclastic carbonate. Frequently, the veins are folded and boudinaged with structures that indicate that the weak foliation (Fig. 4) is oriented parallel to the axial surface. Heterogeneously distributed grain sizes in the matrix define a shape fabric with an aspect ratio of 1:1.5 or less. Calcite grains sometimes display regularly spaced twins, but dynamic recrystallization textures have not been found.

Type II microstructures

Type II microstructures are mainly developed in areas characterized on a mesoscopic scale by a well-developed foliation defined by grain shape that anastomoses around low-strain zones. These rocks generally contain abundant kinematic indicators (Fig. 3) and sheared fossils. Type II microstructures are characterized by a heterogeneous grain size (e.g. samples SSZ2, SSZ4, DB95-18, DB95-21, DB97-1 and DB97-17), where it is possible to identify host grains of a wide range of sizes (2000–100 μm) and dynamically recrystallized grains with an average grain size of *c.* 40 μm. Both parent and recrystallized grains are elongate, with host grains having an aspect ratio of typically 1:2.5, whereas the recrystallized grains have a slightly smaller mean aspect ratio of 1:2 (Fig. 5a). In DB95-21, elongate grains have straight boundaries parallel to the mylonitic foliation and serrate boundaries normal to it (Fig. 5c). In SSZ4 and DB95-18 individual elongate recrystallized grains are generally oblique to the main macroscopically defined mylonitic foliation, displaying asymmetric core and mantle structures (Fig. 5b). Dynamic recrystallization is

Fig. 3. Photograph of a δ-type shear sense indicator in the calc-mylonites of the Zilair Thrust zone. Mantled porphyroclast indicates a top to the WSW (sinistral) shear sense. Mylonitic foliation and bedding are subparallel.

Fig. 4. Photograph of a cataclasite vein that is folded and boudinaged by the mylonitic foliation (axial surface trace is shown by a dashed line). Sparitic cement fills the voids that formed during the brittle deformation (white).

indicated by the presence of new grains developed near host grain boundaries. In the larger calcite grains, Type II and III mechanical twinning (following the classification of Burkhard (1993)) is widespread. These grains show evidence of twin boundary migration as a mechanism of dynamic recrystallization, especially where two twinning systems intersect (Fig. 5b). These twins are characteristic of a deformation temperature below 200 °C. Rarely, thick twins are sheared along grain boundaries in lamellar crystals (Fig. 5a). Twins within twins, and several sets of twins in a single crystal, are also common. Very fine-grained new grains commonly occur between two generations of *e*-lamellae sets (Fig. 5b), or surrounding lamellar crystals that display evidence of twin boundary migration. These microstructures suggest a relation between new small grains and twin boundary migration (e.g. Rutter 1995). In some lamellar grains the net slip between lamellae has a rotation component, and consequently the new grain may have a different lattice orientation from the host grain. Progressive misorientation of the contiguous lamellae is recorded by progressive rotation of the diffraction band pattern in an opposite sense to the general shear displacement and has been detected by electron backscatter diffraction (EBSD) measurements in the SEM. The displacement of mylonitic layering with indented contacts (Fig. 5c) and the development of foliation-parallel dark horizontal seams where opaque and micaceous material are concentrated (Fig. 5f) suggest that pressure solution was also active to some degree.

Type III microstructures

Type III microstructures appear mainly in high-strain zones at the base of the accretionary complex. They are characterized by fine-grained (*c*. 20 μm to *c*. 40 μm), elongate calcite grains with straight to slightly curved boundaries that define the mylonitic foliation (e.g. DB95-17, JAM95-16, DB97-7 and DB97-8), or as an ultramylonite in which 90–100% of primary grains are recrystallized (Fig. 5e). These mylonites are microstructurally more homogeneous than other types, and consist of very fine-grained calcite (*c*. 5–30 μm) that displays an elongate grain shape fabric (Fig. 5d). For example, in samples DB95-9 and SSZ1 there are homogeneous grain sizes formed by 100% dynamically recrystallized polygonal grains that are slightly

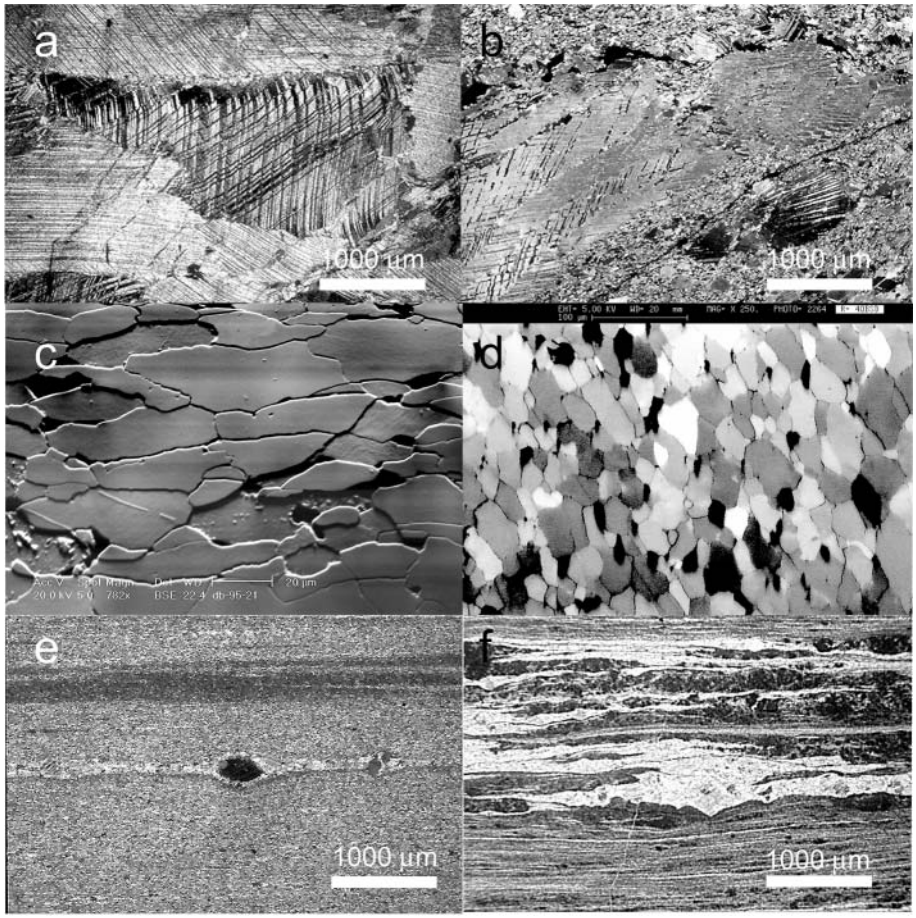

Fig. 5. Photomicrographs showing Type II and III microstructures. For all images the macroscopic foliation is horizontal (except for (**d**), in which it is vertical) and perpendicular to the plane of section. The orientation of the photomicrographs therefore corresponds to that of the pole figures of Figs 6–8. (**a**) Sample DB97-1; note the central lamellar elongate calcite. Its upper boundary is parallel to the mylonitic foliation and shows a biconvex apical twins sheared to the left (west direction). The coarse-grained calcite below has oblique microveins oriented according to the same shear sense. Crossed polars. (**b**) Sample SSZ4; note the lamellar host calcite with twins in twin and high-angle bands of recrystallized grains oblique to the mylonitic foliation and parallel to the boundaries of the host twin set. Another band of recrystallized grains has formed in the neck of the host grain boudin, suggesting a dextral shear sense (west to the right). Crossed polars. (**c**) Sample DB95-21; note that fine grains of the calc-mylonite are elongate parallel to the foliation. Grain boundaries that are perpendicular to the foliation are serrated and display black shadows cast by raised grain edges. SEM backscatter image. (**d**) Sample DB97-7; note that both host and new grains have angular boundaries forming triple points. SEM backscatter electron orientation contrast image suggests crystallographic preferred orientation. (**e**) Sample DB97-4; note that mantle texture developed in the calc-ultramylonite is type ϕ, parallel to the foliation. Crossed polars with gypsum plate inserted. (**f**) Sample DB95-11; note that sparitic veins are folded and boudinaged parallel to the foliation. Pressure solution lamellae mark the mylonitic foliation in the micritic matrix. Plane-polarized light.

elongate (aspect ratio of 1.4–1.5), and that have straight or gently curved grain boundaries. Rarely, small ellipsoidal polycrystalline aggregates (Fig. 5e) have a mantle structure with an associated elongate tail formed by coarser grains than those found in the ultramylonite matrix. Sample DB97-17 has a homogeneous and very small grain size (<20 μm). Because of the fine grain size, mechanical twins are difficult to identify under the microscope (Fig. 5d), but generally seem to be absent.

Locally, there is a variant of the Type III microstructure in which a well-developed cleavage is defined by coarse-grained calcite (>1 mm) intercalated with very fine-grained calcite (<20 μm) in a matrix containing muscovite and chlorite oriented parallel to the foliation. Semi-brittle structures such as veins and boudins, at both meso- and microscopic scale, are common in these zones. For example, in samples DB97-16, DB97-13, DB97-6 and DB97-4, the larger (>70 μm) idiomorphic calcite grains derived from early formed veins that have been subsequently disrupted by shearing contrast with the mylonitic bands of very fine-grained (<14 μm and aspect ratio of *c*. 1:3) polygonal grains that have straight grain boundaries and triple junctions. The coarse grains are partially replaced by chlorite and sericite. An important characteristic of these zones is the abundance of calcite twins, especially in the coarse-grained calcite, where thick *e*-lamellae with prismatic and lenticular twins are found. These grains have microstructural characteristics similar to those described in Type II, but with a higher twin density. Unlike in the Type II microstructure, pressure solution was also active during late stages of the deformation.

Throughout the Timirovo thrust system, coarse-grained fragments of calcite veins form elongate boudins predominantly oriented parallel to the mylonitic foliation (Fig. 5f). In thin section, these veins appear to overprint the early stages of the

mylonitic foliation, but are themselves deformed. Within these veins, mechanical twinning is well developed in all coarse-grained calcite. In samples SSZ3, DB95-12 and DB95-11 core–mantle structures are developed in which dynamically recrystallized fine grains (*c*. 24 μm) form mantles around coarse grains (up to *c*. 3.3 mm). Both fine and coarse grains are slightly elongate, with an aspect ratio of *c*. 1:1.6. In some of these samples, dolomitization and pressure solution appear to have developed at the same time as the mylonitic fabric, especially along the boundaries between coarse- and fine-grained layers. Fine-grained calcite in these locations shows no evidence of internal deformation, and displays the same microstructural characteristics as fine-grained calcite in Type I rocks.

Calcite fabrics

U-stage measurements

Calcite grains from Type I samples show uniform LPO. Calcite grains from Type II and Type III microstructures show marked LPOs that were analysed by U-stage measurements on an optical microscope. Both *c*-axis and the dominant *e*-lamellae orientation were determined in each calcite grain along linear traverses. Optical measurements were carried out using ultrathin sections (<5 μm). Grains from which both *c*-axis and *e*-pole orientations could be analysed by U-stage, and in which both mechanical twins and *c*-axis could be observed together in a single grain, were normally larger than 40 μm. Pole figures of the measured data are shown in Figs 6 and 7. The inverse pole figures (IPFs) show the orientation of the shear plane pole (indicated by the abbreviation Pofo in Figs 6–8) relative to crystal co-ordinates. IPFs of the optical measurements were plotted using the computed symmetrical set of data calculated by unpublished software for construction of calcite crystallographic axes. The macroscopic foliation plane is parallel to the mylonitic foliation at the microscope scale, and given the high strain, the foliation is expected to be close to the shear plane orientation. As calcite has symmetry $-32/m$ it is only necessary to consider the 60° sector (Figs 6 and 7). These stereoplots are useful to characterize low- and high-temperature calcite fabrics (e.g. Wenk *et al*. 1973; Schmid *et al*. 1977; Rutter *et al*. 1994), and occasionally also have been used for naturally sheared calcite mylonites (Schmid *et al*. 1981). Both Schmid's work and this paper present comparable IPFs. The LPOs show progressive and transitional changes from low- to high-strain samples. High strain results in well-defined crystallographic fabrics, whereas low strain results in less well-defined fabrics.

In most of the high-strain pole figures, girdles with concentrations of *c*-axes and *e*-poles around a maximum normal to the foliation plane can be defined (Fig. 6). The lower-strain samples, typified by DB95-21, JAM95-16 and DB95-17, also show some clustering of *c*-axes and *e*-poles near Pofo, but also clearly show single or twin great circle girdles nearly normal to the lineation. From experimental deformation studies, this would be expected of a constrictional fabric developed in the twinning-active deformation regime, with the extension direction parallel to the lineation (Rutter *et al*. 1994). In the higher-strain samples (e.g. DB97-13 and DB97-6, Fig. 6) there is evidence of a remnant of this great circle girdle component.

Low-strain zones (e.g. DB95-21) have a preferred orientation characterized by a pattern of *c*-axes clustered around a great circle perpendicular to the foliation plane and stretching lineation.

These pole figures have a low asymmetry with respect to the foliation plane, with a main maximum parallel to the shear plane pole. The asymmetry, defined as the angle between the shear plane normal and either the *c*-axis maximum or the axis of the small circle girdle of *c*-axes, ranges between 2° (DB97-6) and 15° (DB97-13), but inadequate sampling could lead to the apparent asymmetry in the latter. The pole figures of measured twin lamellae present a maximum subperpendicular to the foliation plane (e.g. DB97-6, DB97-13, DB95-17 and JAM95-16) and they also display complete (low-strain) or partial (high-strain) great circle girdles normal to the lineation. In DB97-13 the orthogonality of the partial great circle girdle with respect to the lineation supports the above interpretation of the apparent symmetry in the *c*-axis pattern. The lack of asymmetry in the LPOs with respect to the foliation plane means that shear sense cannot be inferred from the LPOs. Despite this, shear sense (left-lateral in Fig. 6) was clearly established from macrostructural indicators seen in the field. Other characteristics of these calcite mylonites (both Types II and III) are that the fine-grained samples (<50 μm) show very similar pole figures to the coarse-grained ones (*c*. 200 μm) (Figs 6 and 7).

Electron backscatter diffraction measurements

Electron backscatter diffraction (EBSD) is a modern and widely applicable technique to measure the crystallographic lattice orientation at well-defined locations on the specimen surface with a spatial resolution of about 20 nm and angular resolution of ±0.3° relative to other measurements within the same specimen (Venables & Harland 1973; Dingley & Baba-Kisle 1986; Prior *et al*. 1999). It has been applied as an ideal complementary technique to U-stage measurements in fine-grained calcite, where twin planes (needed for a complete determination of orientation by optical methods) may not be present. In lamellar calcite it is also used to determine the LPO of the lamellae.

For the data reported here, surface charging was reduced by applying a very thin carbon coating. An accelerating voltage of 20 kV and beam currents of about 3 nA were used for EBSD. The acquisition of indexable EBSD patterns was controlled manually, selecting one point from each grain seen on an orientation contrast image (Prior *et al*. 1996). Sample DB95-21 was analysed by both EBSD and U-stage, to compare the results (Figs 6 and 7).

EBSD IPFs are 120° because for complete orientation analysis a non-redundant 120° sector must be considered, whereas U-stage IPFs of 60° allow a better comparison with the results of Schmid *et al*. (1981) and Rutter *et al*. (1994). As with the U-stage measurements, the EBSD IPFs (Fig. 7) also show a progressive development with strain of the *c*-axis maximum parallel to Pofo. Three samples of Type II microstructure (Fig. 5a and b) were analysed. In samples DB95-21 and DB97-17 we measured the lattice orientation of only the fine-grained, recrystallized calcite (*c*. 20 μm) (Fig. 5c), that surrounds the coarse lamellar crystals. In sample DB97-1, we measured recrystallized calcite and the lattice orientation of each lamella of the coarse lamellar crystals. The *c*-axis pole figures show a pattern characterized by a weakly defined great circle girdle normal to the lineation. The *e*-pole figures for DB95-21 and DB97-1 show a distinct tendency to a maximum at Pofo and a weak linking girdle normal to lineation, but for DB97-17 the *e*-pole figure is nearly uniform. No systematic patterns could be discerned for the *r*-pole figures (Fig. 7). Thus, although the pole figures measured by EBSD show the same general characteristics as for those measured by U-stage, they are weaker. This may be a

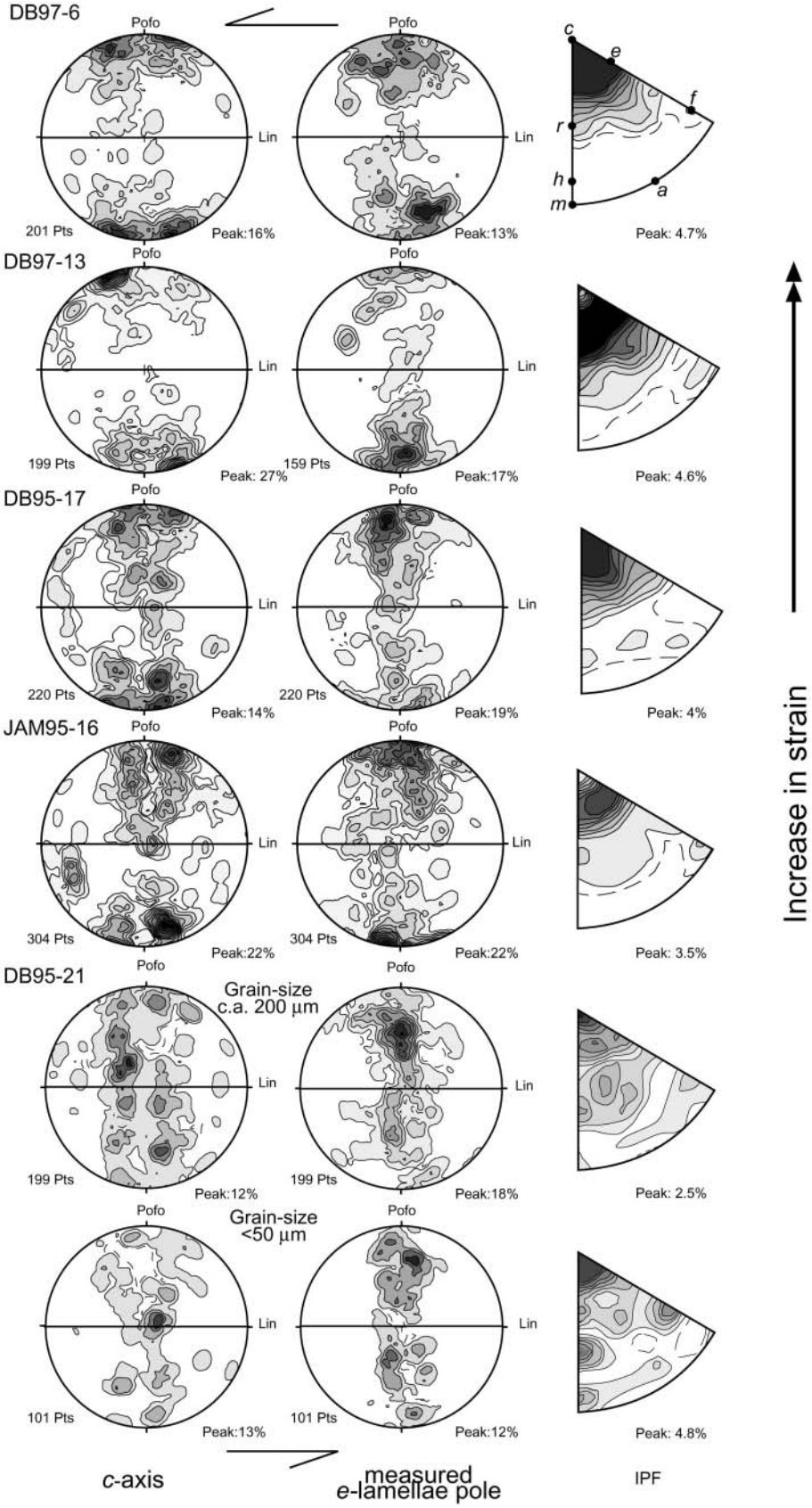

Fig. 6. Pole figures of *c*-axes and *e*-lamellae poles measured by U-stage. The stereoplots are equal area lower hemisphere projections. Contour intervals correspond to multiples of a uniform distribution. The calculation of contour interval uses a 1% search area corresponding to a uniform distribution, where each point represents 0.5%. The lowest contour is 0.5%, the highest contour is the peak, and the contour interval is 2%. The pole figures are presented with the shear plane normal at north and stretching lineation east–west. IPFs represent the poles of foliation (Pofo) relative to crystal co-ordinates. Both lowest contour and contour interval are 0.25%. IPF of sample DB95-18 was also plotted. All pole figures are oriented such that the sense of shear, as inferred from field geological evidence, is sinistral. Sample DB95-21 was plotted in the same form as in Figure 8, to aid comparison of the results.

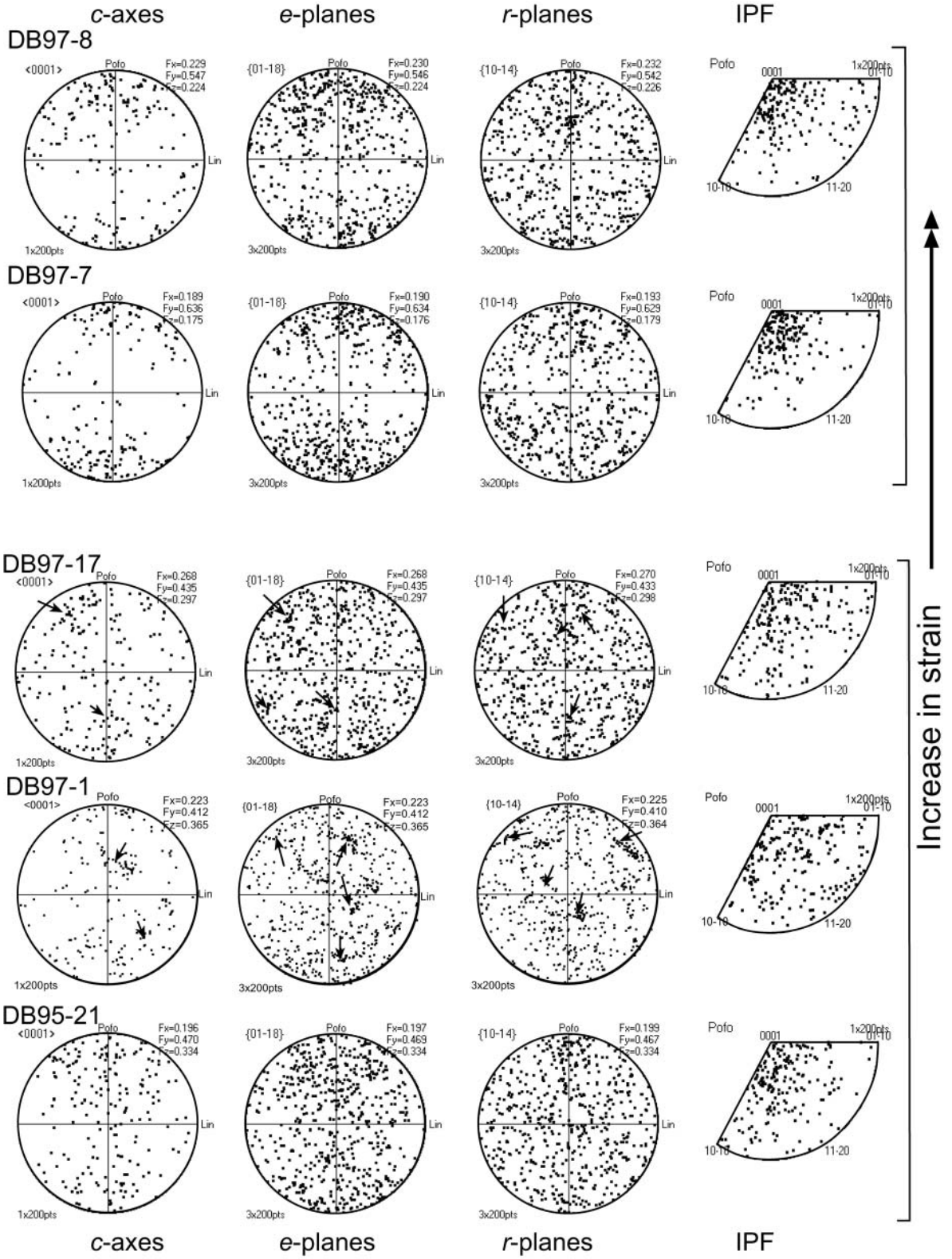

Fig. 7. Crystallographic preferred orientation of fine-grained patch (<50 μm) measured by EBSD. The pole figures are equal area lower hemisphere projections. The pole figures are presented with the shear plane normal at north and stretching lineation east–west. The IPF represents the preferred orientation of poles to the foliation in rhombohedral symmetry. In sample DB97-1 fine recrystallized grains were measured together with lamellar crystals. The orientation of each lamella and recrystallized grains around these lamellar crystals form small circles indicated by the arrows.

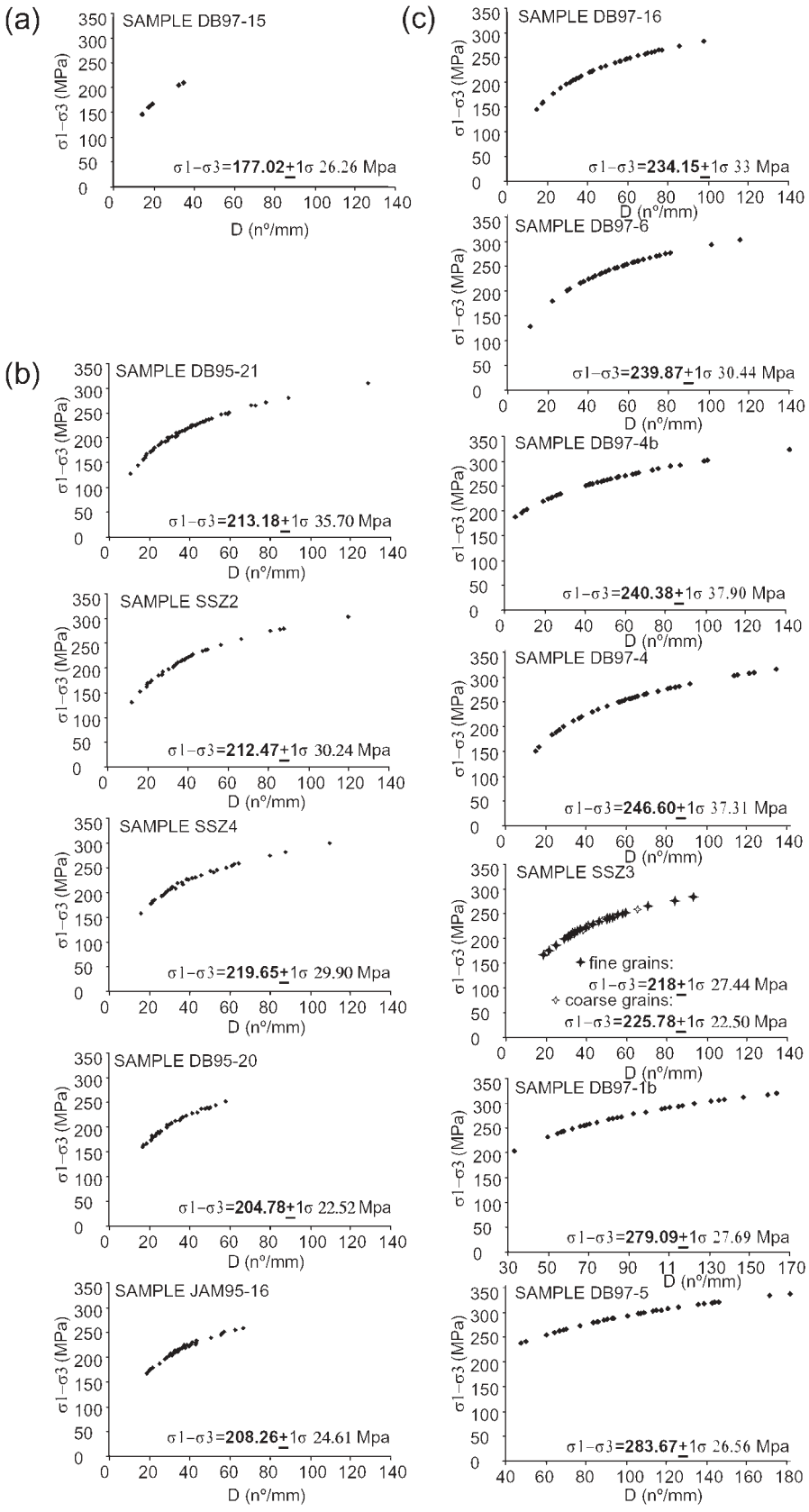

Fig. 8. Palaeostress diagrams. Each point plotted represents the twin density (number of twins per millimetre) per calcite grain analysed. The diagrams are ordered by type of microstructure: (**a**) Type I; (**b**) Type II; (**c**) Type III.

characteristic of the finer, recrystallized grains of the population relative to the coarser parent grains.

Two samples of Type III microstructure were chosen for EBSD analysis (DB97-7 and DB97-8). Both samples consist of fine-grained calcite (*c*. 20 μm) with elongated or equant shapes (Fig. 5d). These have better developed *c*-axis and *e*-pole fabrics. As was observed for similar samples measured by U-stage, these fabrics are characterized by a cluster of *c*-axes and *e*-poles normal to foliation, with a weak remnant of a great circle girdle normal to lineation.

Correlation of LPO with grain shape fabrics

The grain shape preferred orientation in the calcite tectonites studied is distinctly prolate in form, with the grain elongation defining the lineation. This is true of both host and recrystallized grains, although with differences in aspect ratio as described above. Thin sections cut at any orientation parallel to lineation display marked grain shape fabric, yet sections cut normal to lineation show little grain flattening parallel to the trace of foliation. The grain shape fabric suggests a strongly constrictional deformation in the finite strain, and this is consistent with the great circle girdle of *e*-poles normal to lineation described above. On the other hand, the asymmetric shear-sense indicators described above that are seen at the scale of hand specimen and thin section, and the general geological context, also imply that a significant component of rotational strain affected these rocks, probably subsequently to the initial constrictional deformation.

Palaeopiezometry

Several workers have proposed the use of calcite twins as palaeopiezometers (Jamison & Spang 1976; Schmid 1982; Rowe & Rutter 1990). The ideal rock for palaeopiezometry would be a perfectly annealed, pure, homogeneously coarse-grained calcitic marble, lacking LPO, that underwent only minor twinning deformation under very low-temperature conditions (Burkhard 1993). Whether or not twinning occurs in a given grain depends on its orientation with respect to the externally applied stress field. Also, higher shear stresses are required to twin smaller grains. The Rowe & Rutter (1990) palaeopiezometer allowed analysis according to the different grain size class intervals for a single rock specimen, thereby spanning the grain size range 5 μm–1.2 mm for the samples they used. Twinning palaeopiezometry gives only the maximum shear stress to which the sample was ever exposed, and this may be considerably higher than the regionally applied average shear stress. Shear stress can be occasionally intensified if a given rock volume is exposed to local geometric effects such as bending around an asperity on a fault plane. In the latter case, shear stress will appear to decrease with distance from the fault plane.

Calc-mylonites of the Timirovo thrust system have heterogeneous grain size distribution, and deformation occurred in the twinning regime at temperatures high enough for twin boundary migration and rotation. Accordingly, results obtained from palaeopiezometers in these rocks must be regarded with caution. They do, however, show a general increment in stress from microstructural Type I to Type III. As lamellar calcite grains from the Timirovo thrust system show predominantly Type II and III twins of Burkhard (1993), characteristic of temperatures higher than 200 °C, and finite strain is high (inferred to be more than 600% extension), the Rowe & Rutter (1990) palaeopiezometer is the most appropriate (Burkhard 1993; Ferrill 1998). Twin density is here defined as the rate of change of the number of lamellae of a given twin set with respect to grain diameter measured normal to the trace of the twin lamellae, and it was calculated only on grains with more than 10 twins per grain. Submicroscopic twins have not been considered. Only Type II twins of Burkhard (1993) were considered. These twins are thick lamellae with straight and parallel boundaries regularly spaced in the twinned calcite. When possible, at least 100 grains per sample were measured and differential stress was defined for each grain, leading to the determination of a mean value for each sample (Fig. 8).

Sample DB97-15, which has a Type I microstructure, displays rare twinning that gives a low differential stress (*c*. 175 MPa). Twinned grains from Type II microstructure (JAM95-16 and DB95-20) give a slightly higher differential stress (205 MPa), although samples DB95-21, SSZ2, and SSZ4 provide still higher values (*c*. 215 MPa). Twinned grains from Type III microstructure (DB97-16, DB97-6 and DB97-4) present the highest differential stress (*c*. 235 MPa). The differential stress calculated from twinned grains in sample SSZ3, a Type III microstructure cut by a coarse-grained vein, provides values of 218 MPa for fine-grained calcite and 225 MPa for coarse-grained calcite. Especially high differential stress values have been calculated from samples DB97-1 and DB97-5 (*c*. 280 MPa). Both samples contain coarse-grained vein calcite.

Discussion

During the emplacement of the southern Urals accretionary complex onto the East European Craton continental margin, the underlying Devonian limestones were sheared and underplated beneath the frontal part of the prism (Brown *et al*. 1998; Álvarez-Marrón *et al*. 2000). The outcrop observations indicate heterogeneous deformation distributed in a 300–500 m wide band beneath the Zilair Thrust. Shear bands of metre scale with planar and undulatory margins and irregularly developed foliation are distributed within this zone. Veins are very common in less deformed bands, and can be recognized as thin bands of thicker calcite grains within the highly deformed bands. The heterogeneous deformation produced characteristic microstructures and crystallographic orientations of shear-related rocks from lower- to higher-strained zones that we generically define as calcite mylonites.

Deformation mechanisms and fabric development

The calcite mylonites discussed in this paper have been classified according to outcrop and microstructural characteristics into three basic types to facilitate their description and analysis, but transitions between these types are common. Type I corresponds to the less deformed limestone, which contains cataclasite bands, veins and, at times, preserved sedimentary fabrics.

There is a progressive development of LPOs from the low-strain Type II to the high-strain Type III mylonites, where *e*-twinning is revealed as one of the most important operative mechanisms. The pole figure pattern for coarse-grained samples measured by U-stage (Fig. 6) is similar to but more intense than the pattern for fine-grained, recrystallized grains measured by EBSD (Fig. 7). Results from both techniques are broadly comparable, despite some minor differences in the *c*-axis and *e*-lamellae pole figures of sample DB95-21. These differences can be explained to some degree by the mechanical constraints of the U-stage for measuring the orientations of high dip planes. All pole figures, with the exception of the *r*-pole figures (Fig. 7), show a progressive tendency with increasing strain towards axial

symmetry with a *c*-axis maximum normal to the pole to foliation. The *c*-axis and *e*-lamellae pole figures also display a great circle girdle normal to the lineation, which decreases in intensity with increasing strain. Consequently, the pole figures do not present asymmetry that might be related to shear sense. This type of pattern has been described from epizonal tectonites of other regions (Dietrich & Song 1984; De Bresser 1989; Ratschbacher *et al*. 1991).

The grain shape preferred orientation in these tectonites is dominantly prolate in form, with the grains elongate parallel to the lineation. Although we recognize the geometric difficulties of producing a non-plane strain deformation in a localized high-strain zone between relatively undeformed wallrocks, the grain shape fabric suggests a constrictional deformation. This is consistent with the occurrence of the *c*-axis and *e*-pole great circle girdle normal to lineation, which appear to have been produced in the initial stages of deformation, but progressively disappear with increasing strain. This initial type of fabric is readily produced in low-temperature deformation experiments under uniaxial extension when deformation twinning is active (Rutter *et al*. 1994). Only small strains (a few tens of per cent extension) are required to produce a strong fabric, owing to the large reorientation undergone by the twinned volume. However, the failure of the great circle girdle to persist to high strains suggests that the initial constrictional deformation rapidly gives way to other mechanisms or strain increments that give rise to a different LPO (the *c*-maximum normal to Pofo) but without markedly changing the grain shape fabric.

The characteristic types of LPO described in this paper also can be predicted with polycrystal plasticity theory, using combinations of mechanical twinning and intracrystalline slip (see reviews by Wenk 1985, 1998). The topological domain E of Takeshita *et al*. (1987) for the viscoplastic ($r-$, e^+, r^+, $f-$) self-consistent texture simulations of calcite most closely models the low-strain LPO in low-temperature conditions. In this model, the activity of e^+ is about equal to the sum of the activities on $r-$ and $f-$ because shortening and extension along the *c*-axis are geometrically necessary. However, the importance of twinning decreases at high deformation because twinned grains are rarely in a favourable orientation to twin again, and in consequence increasing activity on the $r-$ slip system is predicted. If $r-$ activity increases a softening effect may be expected, slightly more significant in pure shear, whereas a hardening effect caused by the reduced activity of twinning would be expected if the activity of the other slip system cannot accommodate the continued deformation (Wenk *et al*. 1987). We suggest that the imprint of cataclasis on the calcite tectonites of the Timirovo thrust system could result from the hardening effect of the reduction in twinning activity with progressive strain, together with the influence of other factors such as episodic elevation of pore fluid pressure along the thrust system.

Microstructures present in Type II and III samples contain patches of coarse elongated grains dispersed in a very fine-grained matrix that covers more than 90% of the area. At this high strain level, recrystallization has strongly overprinted the original microstructure. Host calcite grains in Type II also show evidence of twin boundary migration (a process of dynamic recrystallization), especially evident where two twinning systems intersect. Additionally, nuclei of recrystallized grains can be produced by grain boundary bulging or subgrain rotation. As most porphyroclasts have not only been sheared but partially consumed by recrystallization, their dimensions have been reduced and their shapes have become more rounded. Very small new grains commonly occur in host-grain material between two generations of *e*-lamellae sets (Fig. 5b), or surrounding lamellar crystals that display evidence of twin boundary migration. These microstructures suggest a relation between new small grains and twin boundary migration (e.g. Rutter 1995). The recrystallized microstructure progressively becomes more homogeneous with a grain size range between 5 and 40 μm.

In addition to these general characteristics, sample DB97-1 displays second-order orientations of the *c*-axes, and *e*- and *r*-poles around rotation axes that give small circle distributions (Fig. 7). These small circles have been interpreted to result from continuous increments of misorientation of the new subgrains formed by rotation around a host grain in one defined position (Canova *et al*. 1984; Gottstein & Shvindlerman 1999; Leiss & Barber 1999). Grain boundary migration is, however, the dominant mechanism of recrystallization.

LPOs of the most highly strained bands show a well-developed fabric in both fine- and coarse-grained calcite (Type II calc-mylonite in Figs 6 and 8) and suggest that in these fabrics dynamically recrystallized grains are also deformed by intracrystalline plasticity in a continuous process. These initially sub-equant, new grains appear to have developed elongated shapes, sometimes with formation of mechanical twins (Fig. 5e) and eventually with the development of a new generation of recrystallized grains (Fig. 5d). In spite of their near homogeneous aspect ratio these grains have a crystallographic preferred orientation, which is inferred to be continuously maintained by increments of intracrystalline plastic strain before the next cycle of recrystallization.

In tectonites as fine grained as these, a contribution to strain is also to be expected from grain boundary sliding (GBS) after the first cycle of grain refinement by dynamic recrystallization. Rutter *et al*. (1994) and Rutter (1995) showed that a wide regime of deformation by a mixture of GBS and intracrystalline plasticity exists for calcite rocks, in which the formation of a strong shape fabric in individual grains with progressive strain is inhibited, whereas the intracrystalline plastic strain component preserves and enhances the LPO and may lead to further cycles of dynamic recrystallization. These processes are likely to have led to the microstructures and fabrics seen in the rocks studied.

An unexpected result of this study is the low asymmetry of all the pole figures (Figs 6 and 8) with respect to the foliation plane. Particularly at high strains, IPFs show a concentration of the Pofo around the crystallographic position of *c* and *e*. This type of IPF is common in experimental deformation studies on calcite rocks and is produced during axisymmetric shortening normal to the foliation defined by grain flattening. In this case the symmetry axis is also the direction of maximum compressive stress, and it is known that the fabric can survive a cycle of dynamic recrystallization (Rutter *et al*. 1994). As well as in the case of the Timorovo samples, the same fabric type has been observed, for example, by Schmid *et al*. (1981) in calcite mylonites from the Helvetic Nappes. It is tempting to interpret the lack of LPO asymmetry in terms of coaxial (irrotational) deformation, by analogy with experimental studies.

Two possible causes have been argued to explain this feature for limestone deformed to high shear strains. Ratschbacher *et al*. (1991) and Erskine *et al*. (1993) studied strongly deformed tectonites in the Craz Palaeozoic thrust sheet (Austria) and in the western USA, respectively, and have suggested that the above-described ‘texture softening’ of Wenk *et al*. (1987) may induce local instabilities in ultramylonite zones whereby smaller volumes of the movement zone may follow coaxial paths, whereas the bulk deformation may approximate to simple shear. This explanation necessarily leads to a strain-path partitioning.

On the other hand, Pieri *et al*. (2001) produced a very sharp and symmetrical single *c*-maximum LPO normal to foliation in Carrara marble experimentally deformed to high shear strain in torsion, and showed how dynamic recrystallization and LPO development can be related to strain softening processes during high-strain deformation. The orthorhombic or axial symmetry for large shear strains is explained because the structural reference frame (foliation and lineation) is close to the kinematic frame, and easy glide can take place on one or more slip systems with a resultant slip vector parallel to the basal plane. In experiments carried out by Casey *et al*. (1998) on a fine-grained limestone deformed to high strains in torsion, similar symmetrical LPOs were obtained, suggesting that the patterns we have observed are characteristic of high-strain simple shear deformation of calcite rocks in nature. Thus axisymmetric LPO types are not necessarily incompatible with rotational deformations.

Deformation conditions

Calcite mylonites within the Timirovo thrust system display a variety of microstructures that indicate deformation conditions that range from semi-brittle to plastic. Lamellar calcite grains from the Timirovo thrust system display predominantly Type II and III twins of Burkhard (1993), argued to be characteristic of temperatures higher than 200 °C. If the twin geometry is truly indicative of this range of temperature, the differential stress measurements obtained from suitable calcite grains give at this temperature a range of values from 175 to 280 MPa, although most of the data range from 215 to 235 MPa. This range of differential stress is commensurate with the level of uncertainty associated with the method, hence it is probably best to regard these rocks as preserving evidence for peak differential stresses of *c*. 230 ± 40 MPa. High differential stresses are also suggested by the small size of recrystallized grains and the small size of abundantly twinned grains (Schmid 1982; Rowe & Rutter 1990; Rutter 1995).

Although bearing in mind the large uncertainties associated with differential stress estimates from twinning, there does seem to be an apparent systematic increase in palaeostress with increasing grain size shown by all samples in Figure 8. Although it is possible that stress is partitioned to some degree into grains of different sizes, it seems unlikely that this happens to the degree implied. Under the conditions of the experiments for which this method was devised the stresses would be constant for the twinning activity observed in each grain. Thus the observed apparent variation probably points to a difference in behaviour between that under the natural conditions of temperature and strain rate and the experimental conditions. Hence the differences in average stresses found for the different samples are not likely to be significant.

Total recrystallization of calcite rocks, such as occurs in our high-strain samples to produce mylonites of a grain size range of between 5 and 40 μm, seems to occur at high stress levels (220 MPa or more), at temperatures higher than 200°C. In these conditions, both twinning and intracrystalline slip are likely to be important in the initial deformation of a coarse-grained protolith. The recrystallized grain sizes are consistent with experimental migration recrystallization data (Rutter 1995) and with the hypothesis that the maximum grain size preserved is delimited by the twinning field boundary.

Conclusions

Calcite deformation fabrics at the base of the southern Urals accretionary complex formed in localized zones of ductile to semi-brittle deformation. Outcrop observations, microstructural variations and crystallographic orientations showed that the deformation was heterogeneous. Microstructural studies showed that mechanical twinning was an important contributor to bulk deformation of the limestones, giving way at higher strains to dynamic recrystallization to a finer-grained mylonitic texture. Grain boundary and twin bulging and migration is the most frequent mechanism of recrystallization in the samples studied. Pressure solution plays a very minor part in the deformation of these calc-mylonites. The grain shape fabric of the rocks is dominantly elongate, defining a mineral lineation, with only a weak flattening component parallel to the mesoscopic foliation in the rocks, defined by variations in grain size and, in some places, by phyllonitization and/or secondary dolomitization. The grain shape fabric suggests non-plane strain, constrictional deformation.

Differential stress calculations derived from twinned calcite grains, together with the small size of recrystallized grains and the small size of abundantly twinned grains, indicate high differential stress conditions during deformation (*c*. 230 MPa). The form of the twins in the calcite is characteristic of a deformation temperature above 200 °C. In these conditions a progressive development of lattice preferred orientation from the low-strained limestone layers to the highly strained bands was observed. The *c*-axis and *e*-lamellae pole figures display a single maximum or girdle, where the maximum coincides with the foliation normal and the girdle forms normal to the macroscopic mineral lineation in the rocks. The girdle fabric is consistent with uniaxial extension parallel to the lineation, and this was observed to weaken at high strain, when the fabric becomes dominated by the *c*-maximum. The *c*-maximum fabric normal to foliation is typical of calcite rocks deformed experimentally to high strains in simple shear. By analogy with experimental data and visco-plastic self-consistent texture simulations, the LPOs indicate that *e*-twinning and *r*-glide were the major deformation mechanisms leading to the LPO development. A contribution to strain from grain boundary sliding is inferred following grain-size reduction by dynamic recrystallization.

We wish to express our thanks to INDUROT for the use of their facilities, and to R. Menéndez-Duarte for assistance during the acquisition of the strain data using GIS. This work was funded by DGCYT, PB97-1141. The SEM facilities in Liverpool are supported by NERC grant GR311768. Reviews by M. Casey and H.-R. Wenk helped clarify concepts and discussions presented in this paper. We sincerely thank E. H. Rutter for his detailed review, which helped to reconcile the field observations and to better address the targets of the discussion.

References

Álvarez-Marrón, J., Brown, D., Pérez-Estaún, A., Puchkov, V. & Gorozhanina, Y. 2000. Accretionary complex structure and kinematics during Paleozoic arc–continent collision in the southern Urals. *Tectonophysics*, **325**, 175–191.

Bastida, F., Aller, J., Puchkov, V.N., Juhlin, Ch. & Oslianski, A. 1997. A cross-section through the Zilair Nappe (southern Urals). *Tectonophysics*, **276**, 253–263.

Beane, R.J. & Connelly, J.N. 2000. $^{40}Ar/^{39}Ar$, U–Pb, and Sm–Nd constraints on the timing of metamorphic events in the Maksyutov Complex, southern Urals, Ural Mountains. *Journal of the Geological Society, London*, **157**, 811–822.

Brown, D. & Spadea, P. 1999. Processes of forearc and accretionary complex formation during arc–continent collision in the southern Ural Mountains. *Geology*, **27**, 649–672.

Brown, D., Álvarez-Marrón, J., Pérez-Estaún, A., Gorozhanina, Y., Barishez, V. & Puschov, V.N. 1997. Geometric and kinematic evolution of the foreland thrust and fold belt in the southern Urals. *Tectonics*, **16**, 551–562.

Brown, D., Juhlin, C., Álvarez-Marrón, J., Pérez-Estaún, A. & Oilianski,

A. 1998. Crustal-scale structure and evolution of an arc–continent collision zone in the southern Urals, Russia. *Tectonics*, **17**, 158–171.

Burkhard, M. 1993. Calcite twins, their geometry, appearance and significance as stress–strain markers and indicators of tectonic regime: a review. *Journal of Structural Geology*, **15**, 351–368.

Busch, J.P. & van der Pluijm, B.A. 1995. Calcite textures, microstructures and rheological properties of marble mylonites in the Bancroft shear zone, Ontario, Canada. *Journal of Structural Geology*, **17**, 677–688.

Canova, G.R., Kocks, U.F. & Jonas, J.J. 1984. Theory of torsion texture development. *Acta Metallurgica*, **32**, 211–226.

Casey, M., Kunze, K. & Olgaard, D.L. 1998. Texture of Solnhofen limestone deformed to high strain in torsion. *Journal of Structural Geology*, **20**, 255–267.

De Bresser, J.H.P. 1989. Calcite *c*-axis testures along the Gavarnie thrust zone, central Pyrenees. *Geologie en Mijnbouw*, **68**, 367–375.

Dietrich, D. & Song, H. 1984. Calcite fabrics in a natural shear environment, the Helvetic nappes of western Switzerland. *Journal of Structural Geology*, **6**, 19–32.

Dingley, D.J. & Baba-Kisle, K. 1986. Use of electron diffraction patterns of determination of crystal symmetry elements. *Scanning Electron Microscopy*, **II**, 383–391.

Erskine, B.G., Heidelbach, F. & Wenk, H.-R. 1993. Lattice preferred orientations and microstructures of deformed Cordilleran marbles; correlation of shear indicators and determination of strain path. *Journal of Structural Geology*, **15**, 1189–1205.

Ferrill, D.A. 1998. Critical re-evaluation of differential stress estimates from calcite twins in coarse-grained limestone. *Tectonophysics*, **285**, 77–86.

Glodny, J., Bingen, B., Austrheim, H., Molina, J.F. & Rusin, A. 2002. Precise eclogitization ages deduced from Rb/Sr mineral systematics: the Maksyutov complex, Southern Urals, Russia. *Geochimica et Cosmochimica Acta*, **66**, 1221–1235.

Gottstein, G. & Shvindlerman, L.S. 1999. *Grain Boundary Migration in Metals: Thermodynamics, Kinetics, Applications*. CRC Press, Boca Raton, FL.

Jamison, W.R. & Spang, J.H. 1976. Use of calcite twin lamellae to infer differential stress. *Geological Society of America Bulletin*, **87**, 868–872.

Kern, H. & Wenk, H.-R. 1983. Calcite texture development in experimentally induced ductile shear zone. *Contributions to Mineralogy and Petrology*, **83**, 231–236.

Leiss, B. & Barber, D.J. 1999. Mechanisms of dynamic recrystallization in naturally deformed dolomite inferred from EBSP analyses. *Tectonophysics*, **303**, 51–69.

Matte, P., Maluski, H., Caby, R., Nicolas, A., Kepezhinskas, P. & Sobolev, S. 1993. Geodynamic model and 39Ar/40Ar dating for the generation and emplacement of the high pressure (HP) metamorphic rocks in SW Urals. *Comptes Rendus de l'Académie des Sciences, Série II*, **317**, 1667–1674.

Pieri, M., Kunze, K., Burlini, L., Stretton, I., Olgaard, D.L., Burg, J.-P. & Wenk, H.R. 2001. Texture development of calcite by deformation and dynamic recrystallization at 1000 K during torsion experiments of marble to large strains. *Tectonophysics*, **330**, 119–140.

Prior, D.J., Trimby, P.W., Weber, U.D. & Dingley, D.J. 1996. Orientation contrast imaging of microstructures in rocks using forescatter detectors in the scanning electron microscope. *Mineralogical Magazine*, **60**, 859–869.

Prior, D.J., Boyce, A.P., *et al.* 1999. The application of electron backscatter diffraction and orientation contrast imaging in the SEM to textural problems in rocks. *American Mineralogist*, **89**, 1741–1759.

Puchkov, V.N. 1997. Structure and geodynamics of the Uralian orogen. *In:* Burg, J.P. & Ford, M. (eds) *Orogeny through Time*. Geological Society, London, Special Publications, **121**, 201–236.

Ratschbacher, L., Wenk, H.-R. & Sintubin, M. 1991. Calcite texture: examples from nappes with strain-path partitioning. *Journal of Structural Geology*, **13**, 369–384.

Rowe, K.J. & Rutter, E.H. 1990. Palaeostress estimation using calcite twinning: experimental calibration and application to nature. *Journal of Structural Geology*, **12**, 1–17.

Rutter, E.H. 1974. The influence of temperature, strain rate and interstitial water in the experimental deformation of calcite rocks. *Tectonophysics*, **22**, 311–334.

Rutter, E.H. 1995. Experimental study of the influence of stress, temperature and strain on the dynamic recrystallization of Carrara marble. *Journal of Geophysical Research*, **100**, 24651–24663.

Rutter, E.H., Casey, M. & Burlini, L. 1994. Preferred crystallographic orientation development during the plastic and superplastic flow of calcite rocks. *Journal of Structural Geology*, **10**, 1431–1446.

Savalieva, G.N., Sharashin, A.Y., Sveliev, A.A., Spadea, P. & Gaggero, L. 1997. Ophiolites of the Southern Uralides adjacent to the East European Continental Margin. *Tectonophysics*, **276**, 117–138.

Schmid, S.M. 1982. *Laboratory experiments on rheology and deformation mechanisms in calcite rocks and their application to studies in the field*. Zurich, ETH und der Universität Zürich, Mitteilungen aus dem Geologischen Institut, Neue Folge, **241**.

Schmid, S.M., Boland, J.N. & Paterson, M.S. 1977. Superplastic flow in fine grained limestone. *Tectonophysics*, **43**, 257–291.

Schmid, S.M., Casey, M. & Starkey, J. 1981. The microfabric of calcite tectonites from the Helvetic Nappes (Swiss Alps). *In:* McClay, K.R. & Price, N.J. (eds) *Thrust and Nappe Tectonics*. Geological Society, London, Special Publications, **9**, 151–158.

Schmid, S.M., Pannozzo, R. & Bauer, S. 1987. Simple shear experiments on calcite rocks: rheology and microfabrics. *Journal of Structural Geology*, **9**, 747–778.

Takeshita, T., Tomé, C., Wenk, H.-R. & Kocks, U.F. 1987. Simple-crystal yield surface for trigonal lattices: application to texture transitions in calcite polycrystals. *Journal of Geophysical Research*, **92**, 917–12930.

Turner, F.J., Griggs, D.T., Clark, R.H. & Dixon, R.H. 1956. Deformation of Yule marble, part VII: development of oriented fabrics at 300 °C–400 °C. *Geological Society of America Bulletin*, **67**, 1259–1294.

Venables, J.A. & Harland, C.J. 1973. Electron backscatter patterns—a new technique for obtaining crystallographic information in the SEM. *Philosophical Magazine*, **27**, 1193–1200.

Wagner, F., Wenk, H.R., Kern, H., Van Houtte, P. & Esling, C. 1982. Development of preferred orientation in plane strain deformed limestone: experiment and theory. *Contributions to Mineralogy and Petrology*, **80**, 132–139.

Wenk, H.-R. 1985. Carbonates. *In:* Wenk, H.-R. (ed.) *Preferred Orientation in Formed Metals and Rocks. An Introduction to Modern Texture Analysis*. Academic Press, Orlando, FL, 361–384.

Wenk, H.-R. 1998. Typical textures in geological material and ceramics. *In:* Kocks, U.F., Tomé, C.N. & Wenk, H.-R. (eds) *Texture and Anisotropy: Preferred Orientations in Polycrystals and their Effect on Materials Properties*. Cambridge University Press, Cambridge, 240–271.

Wenk, H.R., Venkitasubramanyan, C.S. & Baker, D.W. 1973. Preferred orientation in experimentally deformed limestone. *Contributions to Mineralogy and Petrology*, **38**, 81–114.

Wenk, H.-R., Takeshita, T., Bechler, E., Erskine, B.G. & Matthies, S. 1987. Pure shear and simple shear calcite textures. Comparison of experimental, theoretical and natural data. *Journal of Structural Geology*, **9**, 731–745.

Zonenshain, L.P., Kuzmin, M.I. & Natapov, L.M. 1990. Uralian fold belt. *In:* Page, B.M. (ed.) *Geology of the USSR: a Plate-Tectonic Synthesis*. American Geophysical Union, Geodynamics Series, **21**, 27–54.

Received 25 February 2003; revised typescript accepted 17 June 2003.
Scientific editing by Alex Maltman